Supporting information

Anti-freezing conductive hydrogel with exceptional mechanical properties and stable sensing performance at -30 °C

*Yunfei Yu, Shuo Wang, Huitao Yu, Xiaojian Liao, Wei Feng**

Tianjin Key Laboratory of Composite and Functional Materials, School of Materials Science and Engineering, Tianjin University, Tianjin 300350, P. R. China.

*Corresponding author. E-mail: weifeng@tju.edu.cn (W. Feng)

Experimental Section

Materials: acrylamide (AM) 99.9%, ammonium persulfate (APS) 99.99%, N-dimethylacrylamide (MBA) 98%, and agar were provided by Shanghai Merrill Chemical Technology Co., Ltd. Dimethyl sulfoxide (DMSO) 99.9% was obtained from tianjin Jiangtian Chemical Technology Co., Ltd. Ltd. Deionized water was produced by Senkong Instrument ES-ii-20. All of the materials and chemicals were used as received without any treatment. MXene dispersion (5 mg/mL) was provided by Nanjing Xianfeng Nanomaterial Technology Co. The MXene solution was sonicated for 30 minutes with a frequency of 20 kHz, to disperse MXene nanosheets into a single layer.

Synthesis of the H-MPA: stretchable H-MPA were synthesized through the simple one-pot rapid MXene-catalyzed radical polymerization. First, dried AM (2 g) and a specific concentration of agar (0.05 g, 0.1 g, 0.15 g, 0.2 g, 0.25 g) were successively dispersed into ultrapure water and DMSO solution (10 g, water: DMSO = 5: 5) by magnetic stirring for 20 min at ambient temperature. The obtained mixture was treated in an ultrasonic bath with a frequency of 20 kHz for 1 h at 0 ºC to attain homogeneous suspension. Subsequently, MBA (0.004 g) was added to suspension under vigorous stirring for another 1 h. After 5 degassing cycles with high purity N_2 (≥99.99%), APS (0.1 mol% of AM), and 1 mL MXene dispersion were quickly added under stirring for 1 min. The uniform solution was promptly cast into PTFE 60 mm * 10 mm * 2 mm) molds, where the reaction was carried out at room temperature for 2 minutes.

Synthesis of PAM hydrogels: Stretchable PAM/agar hydrogels were synthesized through the simple one-pot method. First, dried AM (2 g) and agar (0.2 g) were successively dispersed into ultrapure water (10 g, electrical resistance >18.2 MΩ·cm) by magnetic stirring for 20 min at ambient temperature. The obtained mixture was treated in an ultrasonic bath with a frequency of 20 kHz for 1 h at 0 ºC to attain homogeneous suspension. Subsequently, MBA (0.004 g) were added to suspension under vigorous stirring for another 1 h. After 5 degassing cycles with high purity N_2 (≥ 99.99%), APS (0.1 mol% of AM) was quickly added under stirring for 1 min. The uniform solution was promptly cast into PTFE (60 mm X 10 mm X 2 mm) molds.

Polymerization of AM monomer was proceeded in an oven at 60 ºC for 20 h to obtain the PAM/agar hydrogel.

Synthesis of H-PA hydrogels: stretchable PAM/agar hydrogels were synthesized through the simple one-pot method. First, dried AM (2 g) and agar (0.2 g) were successively dispersed into ultrapure water and DMSO solution (10 g, water: DMSO =7: 3; 5: 5; 3: 7; 0:10, respectively) by magnetic stirring for 20 min at ambient temperature. The obtained mixture was treated in an ultrasonic bath with a frequency of 20 kHz for 1 h at 0 ºC to attain homogeneous suspension. Subsequently, MBA (0.004 g) was added to suspension under vigorous stirring for another 1 h. After 5 degassing cycles with high purity N_2 (⩾99.99%), APS (0.1 mol% of AM) was quickly added under stirring for 1 min. The uniform solution was promptly cast into PTFE (60 mm * 10 mm * 2 mm) molds. Polymerization of AM monomer proceeded in an oven at 60 ºC for 20 h to obtain the PAM/agar hydrogel.

Fabrication of the H-MPA based strain sensor: The H-MPA thin films were sliced into rectangular strips. The rectangular strip served as the main sensing material. Two copper wires were tightly linked to both ends of the strip as electrodes to assemble the resistance-type strain sensor.

General characterization: The microstructure of MXene nanosheets was analyzed using AFM by Bruker and Scanning Electron Microscopy (SEM) by Hitachi S-4800. The microstructures of the H-MPA were characterized through Fourier-transform infrared spectroscopy using a Nicolet Nexus 870 and X-ray diffraction analysis with a Shimadzu XRD-6000. The vacuum-dried H-MPA was characterized by IR spectroscopy using a spectrometer (Nicolet Nexus 870) in the attenuated total reflection mode with a scan range of 400–4000 cm^{-1} and a resolution of 4 cm^{-1}. The SAXS device is Xeuss 3.0. Among them, the detector model is Eiger2R 1M, with a pixel edge length of 75 microns; Using copper target 8.05 KeV X-ray with a wavelength of 1.54189 angstroms. Test environment: Vacuum (<1 mbar). Distance from detector to sample: WAXS: 60 mm. Raman spectroscopy tested by Horiba LabRAM HR Evolution. Differential scanning calorimeter (DSC) instrument model: Germany Netsch DSC 200

F3. Atomic force microscope (AFM) instrument model: Bruker Dimension Icon, Germany.

Mechanical tests at room temperature: A universal testing platform (UTM2203, Shenzhen Suns Technology Stock Co., Ltd., China) controlled by a customized computer equipped with a 100 N force sensor was employed to measure the mechanical performances. For the tensile measurement, the uniaxial tests of H-MPA were conducted at a crosshead speed of 30 $mm \cdot min^{-1}$. The elastic modulus of as-prepared gels was calculated from the slope of stress-strain curves within the original linear region.

Electrical measurements at room temperature: The electrical performances of H-MPA sensors were performed with the help of the universal testing machine coupled with a digital multimeter (DMM4050, Tektronix). For the measurement of real-time human movement signals, the H-MPA sensors were adhered to the human skin with the help of commercial adhesive PU tape. Furthermore, Cu electrodes were linked to H-MPA for coinstantaneous detection. The strain-induced response sensitivity was determined using the formula $GF = (R-R_0)/R_0\mathcal{E} = \Delta R/R_0\mathcal{E}$, where R, R_0, and $\mathcal{E}$ are the real-time resistance, initial resistance, and tensile strain of the H-MPA, respectively. This calculation helps assess the sensitivity of the H-MPA to strain-induced changes in resistance. The informed consent with signature was obtained from the volunteer for the human activities experiments. During the experiment, a piece of commercial adhesive polyurethane tape was employed to separate the volunteer's skin surface from the hydrogel based strain sensor, which had no physical or psychological effect on the volunteer. After the experiment, there was no physical or psychological effect on the volunteer. Furthermore, it is important to note that all human volunteers provided informed consent to participate in the study, and ethical approval was not deemed necessary for the research conducted.

Strain sensing tests at -30 ℃: Before the testing, the specimens were stored s in a fridge at -30 ℃ for 24 h. Then the specimens were loaded on lamps vertically in the microcomputer-controlled electronic universal testing machine with a temperature regulation function (Lishi Scientific Instrument Co., Ltd, LD24.104). Meanwhile, the

specimens were connected to the resistance testing instrument (DMM4050, Tektronix) through an external wire while stretching. After the test temperature was stable at -30 ℃, the tests started and the whole process was recorded as shown in Movie S2 and S3.

Rheological test: the rheometer Anton Paar MCR 302 and Australia (Time scan with a fixed strain of 0.5% and frequency of 1 Hz) were used to test the gel transformation time of the solution. The storage modulus and loss modulus of the hydrogel was tested by the same equipment (room temperature, constant strain 0.5%, frequency variation range 0.1-10 Hz).

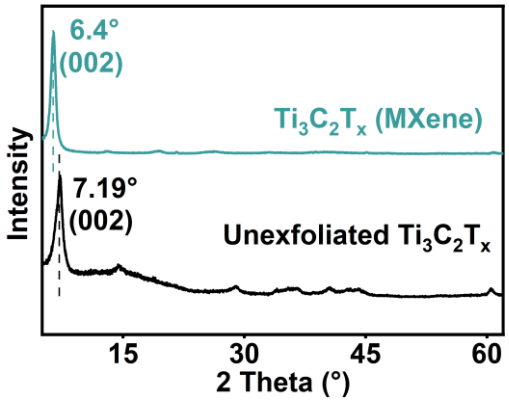

Fig. S1. XRD pattern of unexfoliated $Ti_3C_2T_x$ and $Ti_3C_2T_x$ (MXene).

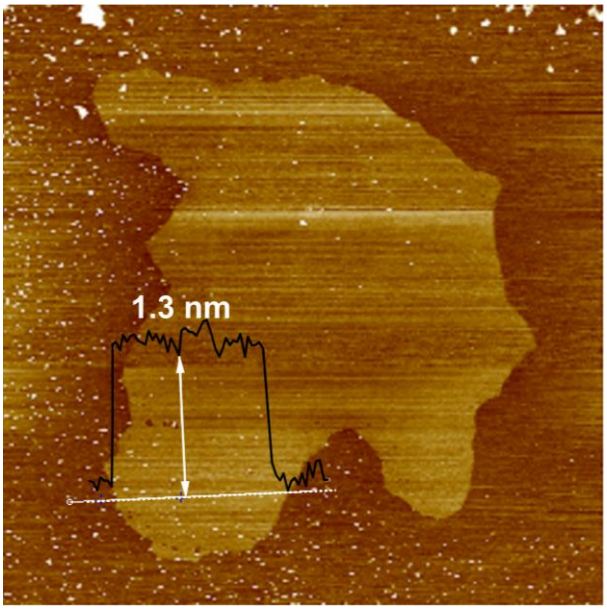

Fig. S2. Atomic force microscope of MXene nanosheets. The internal data line represents the thickness of the scanned MXene nanosheets.

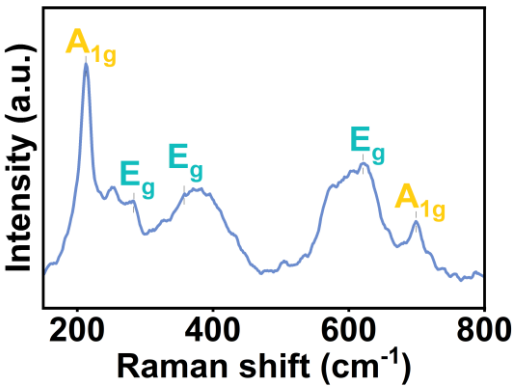

Fig. S3. Raman spectra of MXene nanosheets. The peaks at 212 cm^{-1} and 717 cm^{-1} correspond to A_{1g} symmetric out-of-plane vibrations of Ti and C atoms, respectively. The peaks observed at 284 cm^{-1}, 366 cm^{-1}, and 624 cm^{-1} represent E_g group vibrations associated with in-plane shear modes of Ti, C, and surface functional group atoms respectively.

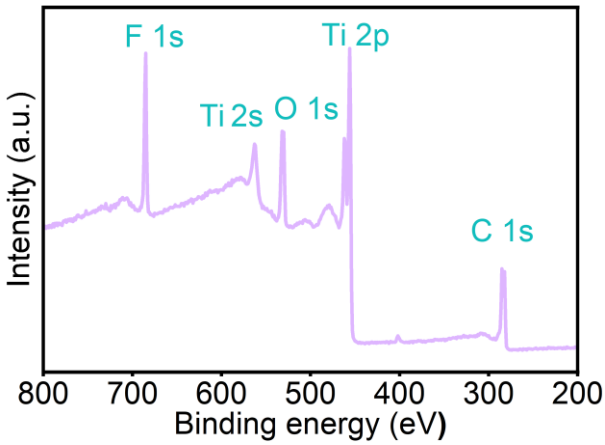

Fig. S4. XPS spectra of MXene with bending energy from 200 to 800 eV.

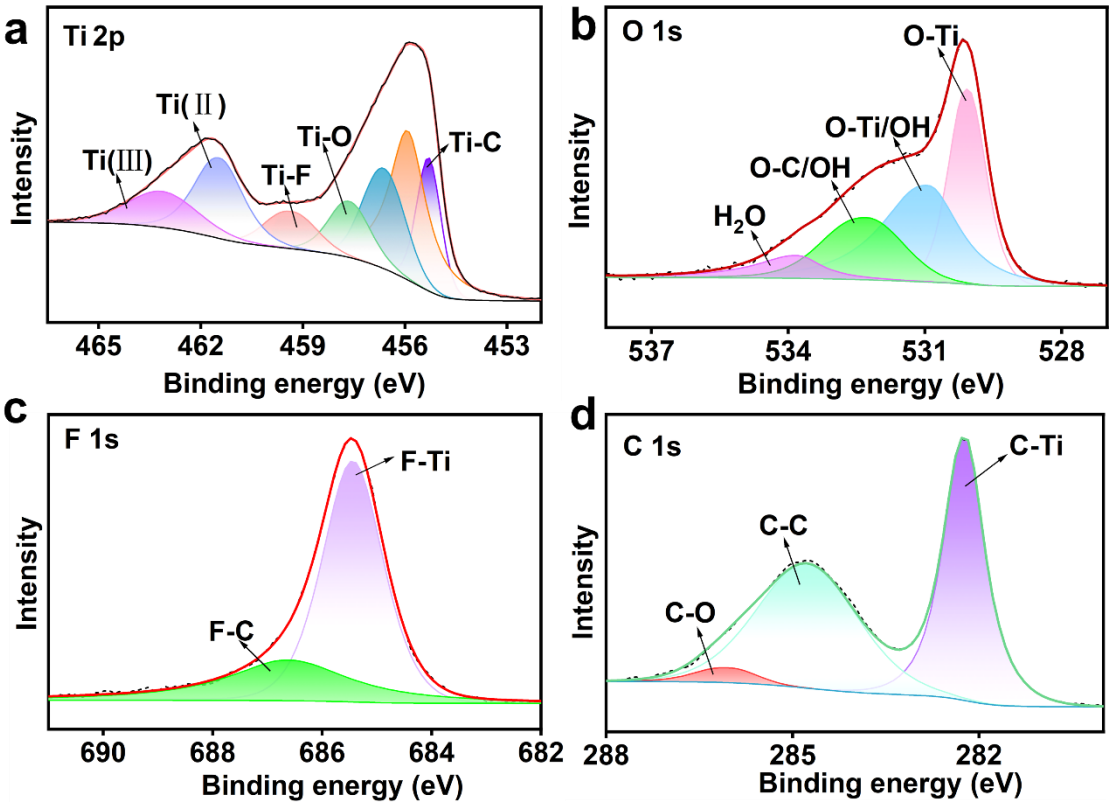

Fig. S5. XPS fine spectra of MXene: (a) Ti 2p; (b) O 1s; (c) F 1s; (d) C 1s.

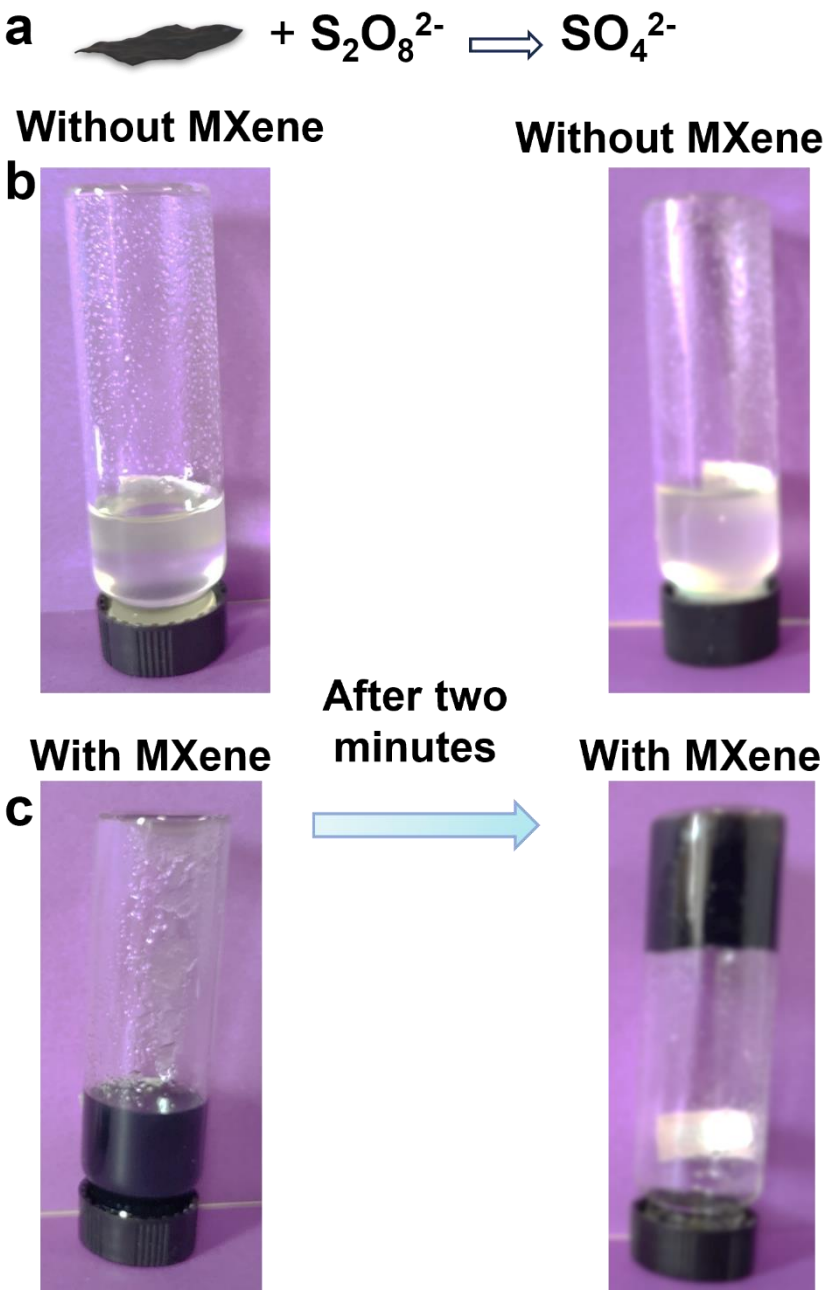

Fig. S6. (a) MXene catalyzed persulfate initiated reaction with a simplified formula, (b-c) Comparison of the physical states of solutions at room temperature before and after polymerization without and with MXene at RT.

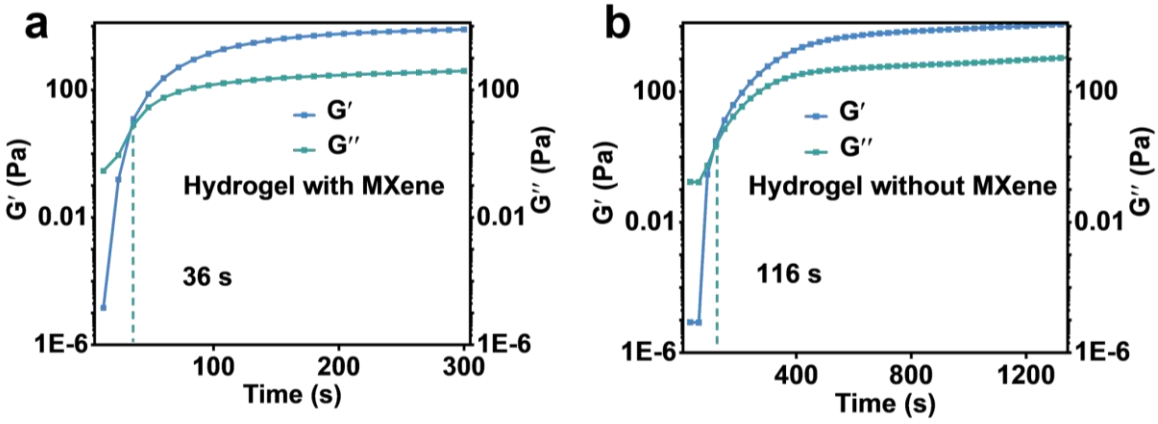

Fig. S7. (a) Rheological testing of hydrogel solutions with MXene at 25 ℃. (b) Rheological testing of hydrogel solutions without MXene at 60 ℃.

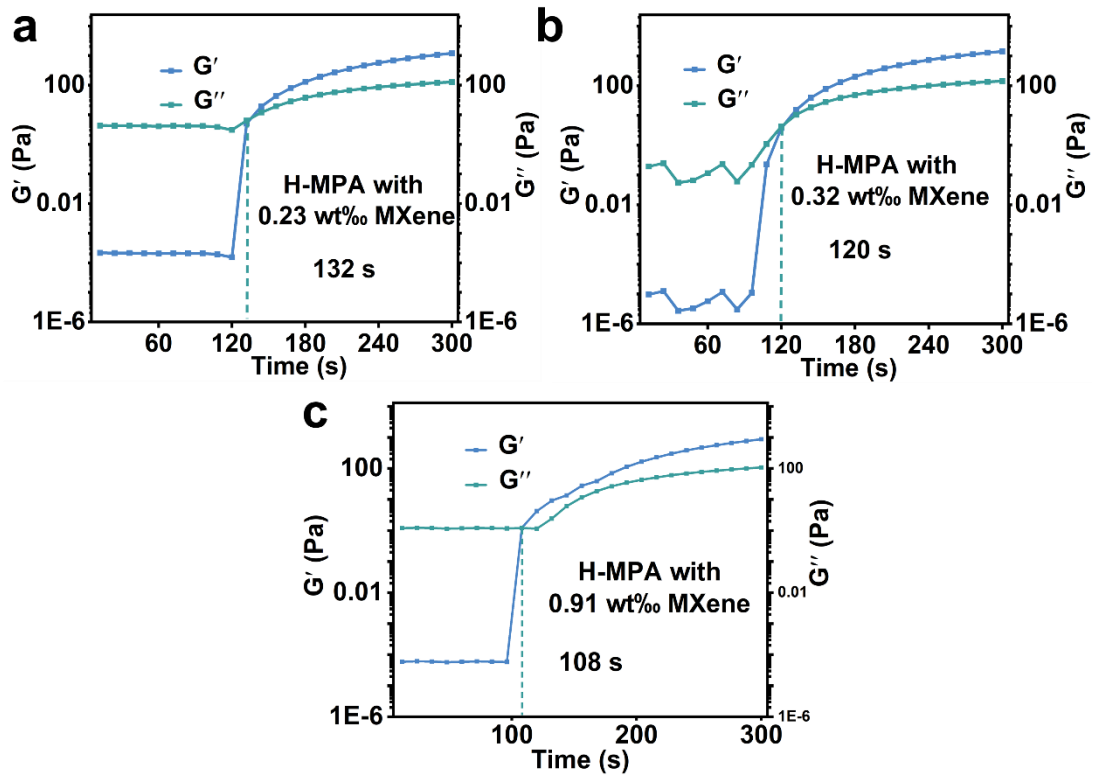

Fig. S8. (a) Rheological testing of H-MPA solutions with 0.23 wt‰ MXene at 25 ℃. (b) Rheological testing of H-MPA solutions with 0.32 wt‰ MXene at 25 ℃. (c) Rheological testing of H-MPA solutions with 0.91 wt‰ MXene at 25 ℃.

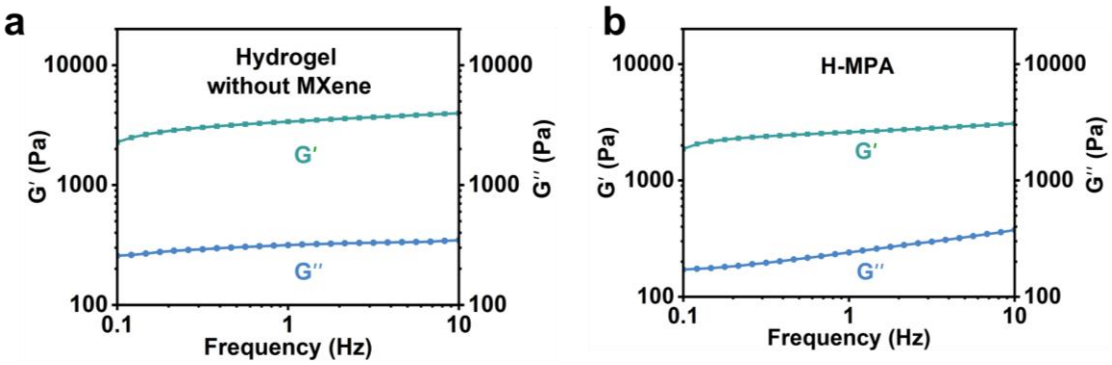

Fig. S9. (a) Rheological properties of hydrogel without MXene at different frequencies. (b) Rheological properties of H-MPA at different frequencies.

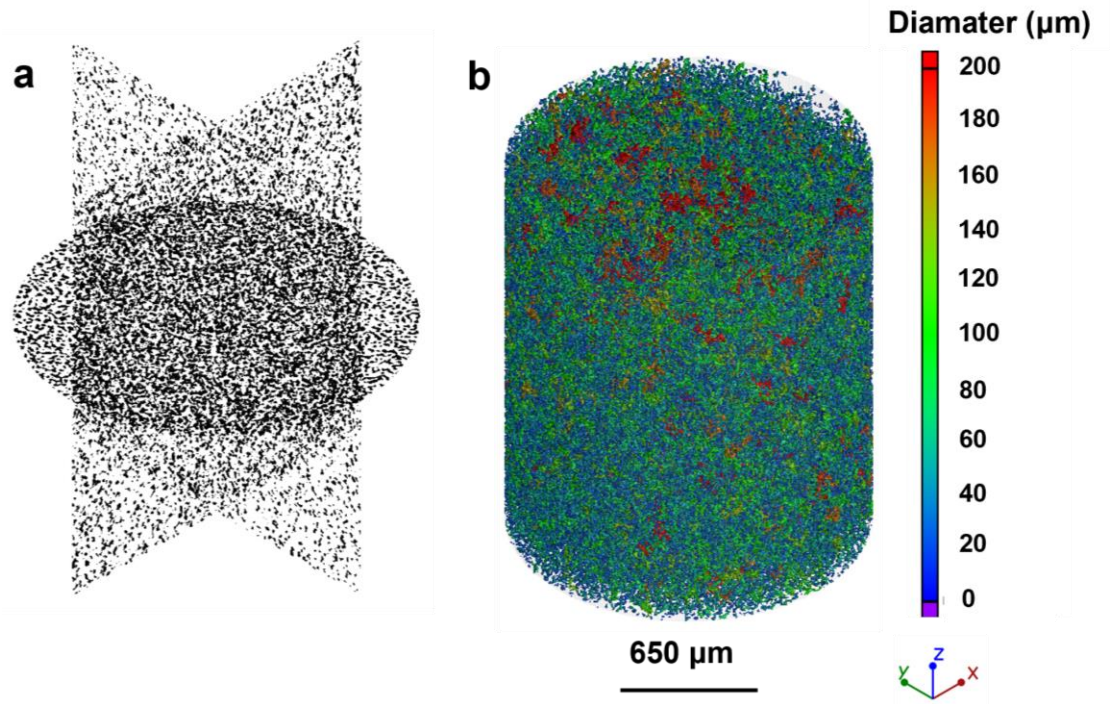

Fig. S10. (a) Two-dimensional plan view of H-MPA reconstructed by CT, (b) H-MPA 3D model reconstructed by CT and its aperture distribution.

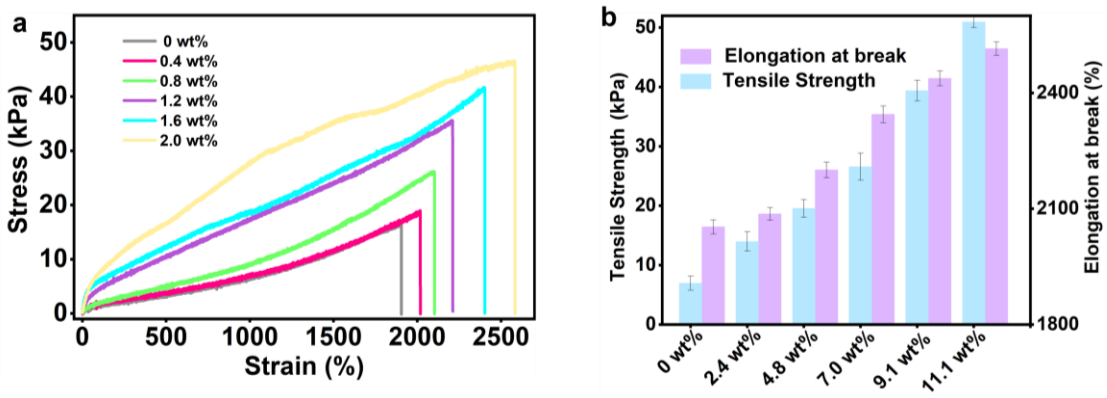

Fig. S11. (a) Stress-strain curves of the H-MPA with different agar contents. (b) Statistics of the typical mechanical properties of H-MPA with different agar contents.

Fig. S12. Digital photos of the hydrogels after reaction with agar content of 15 wt%. With a further increase in agar content up to 15 wt%, the physical network structure of agar dominates within the H-MPA, hindering the reaction of PAM chains and resulting in brittle reactants that fail to exhibit desirable mechanical properties.

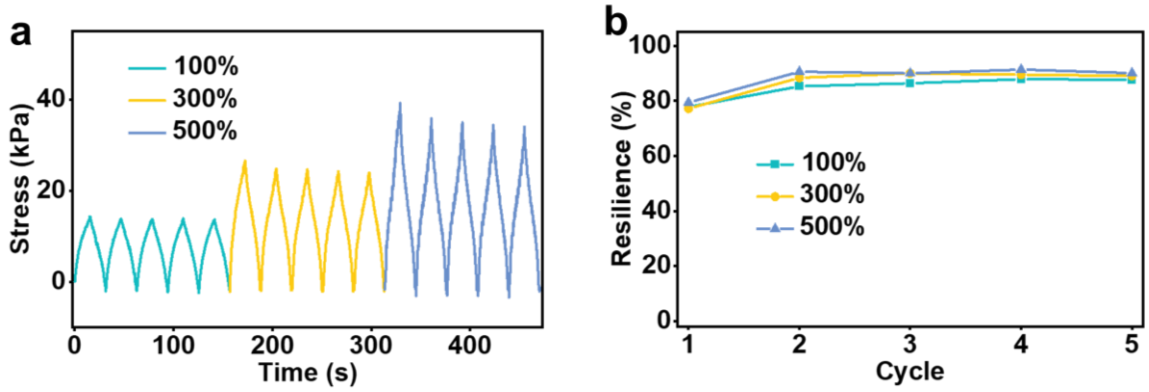

Fig. S13. (a) Stress changes of the H-MPA with time under 100%, 300%, and 500% strain. (b) Strain recovery statistics of the H-MPA after five cycles under 100%, 300%, and 500% strain.

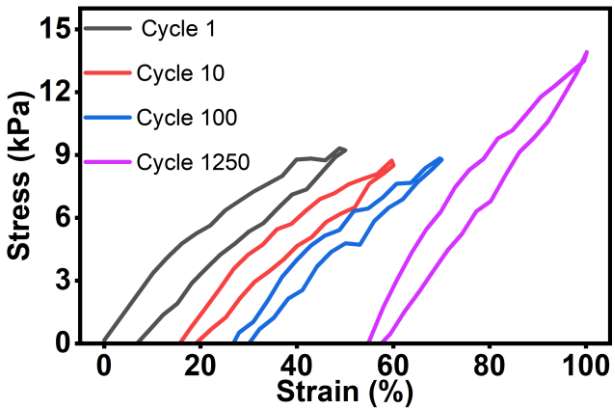

Fig. S14. Stress-stain curves during cyclic tests at different cycles.

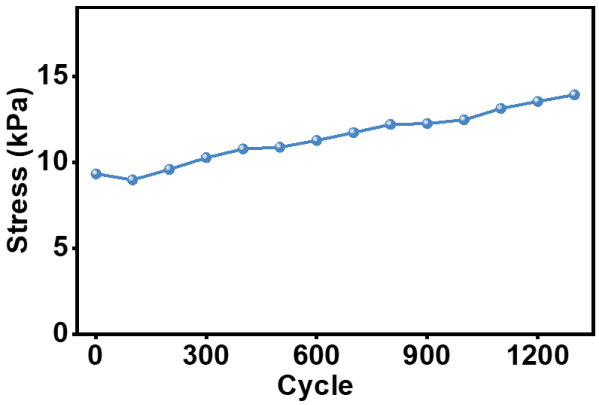

Fig. S15. Maximum stress statistics of H-MPA after 1250 cycles under 50% strain.

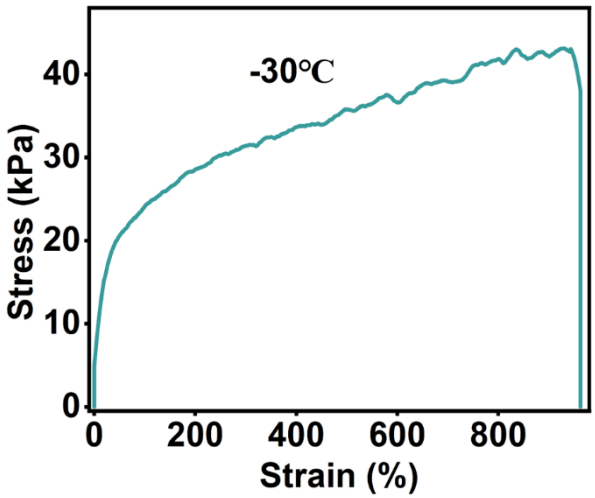

Fig. S16. Stress-strain curve of the H-MPA at -30 ℃.

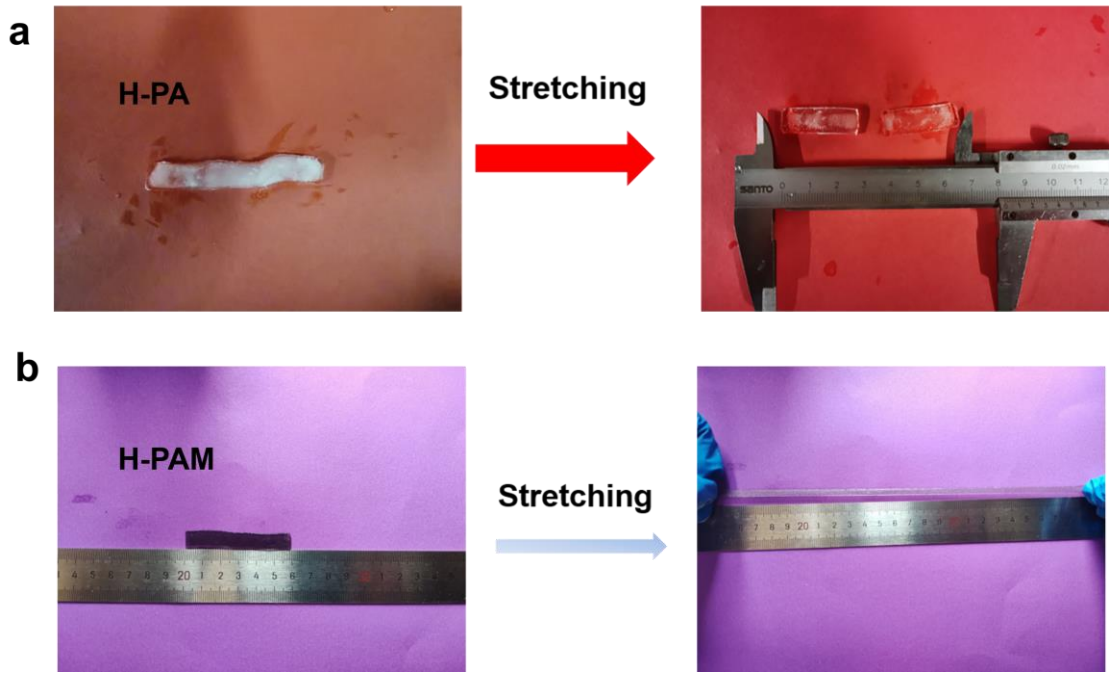

Fig. S17. (a) Digital photographs of H-PAM in a low-temperature state and under tension, respectively. The H-PAM fractures during the stretching processing at low temperatures. (b) Digital photographs of H-MPA in a low-temperature state and under tension, respectively. The H-MPA was stretched by 6 times without fracture at low temperatures.

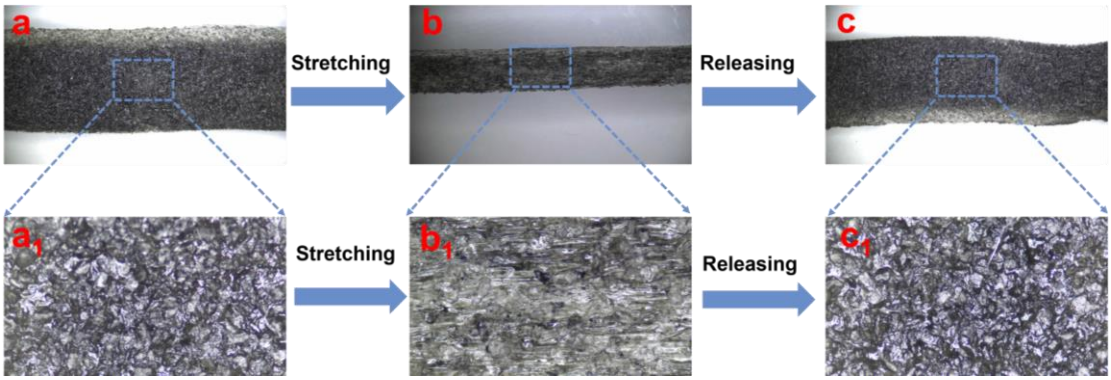

Fig. S18. The optical microscope images of the H-MPA in the initial state, stretched state, and recovered state to the initial state: (a) original length state; (b) stretching to 200% strain; c) restoring to original length state.

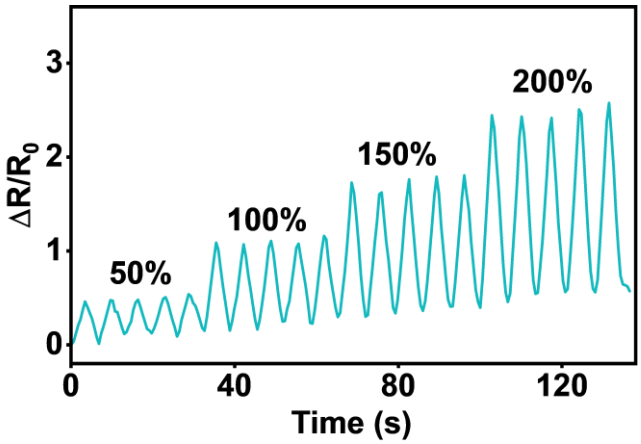

Fig. S19. Changes of the resistance variation with time in H-MPA at different strains.

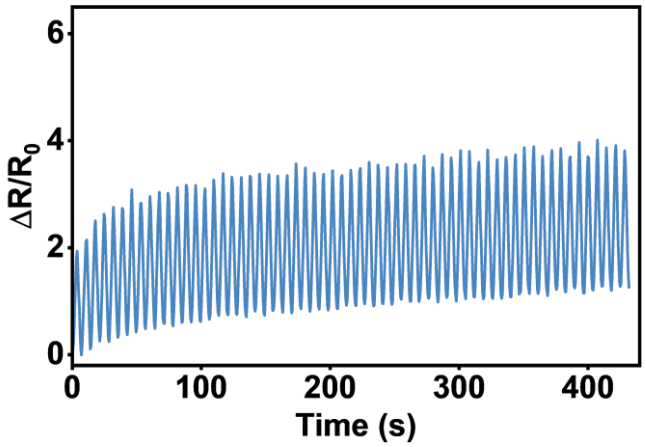

Fig. S20. Changes in the resistance variation with time in H-MPA during 60 cycles test at 200% strain.

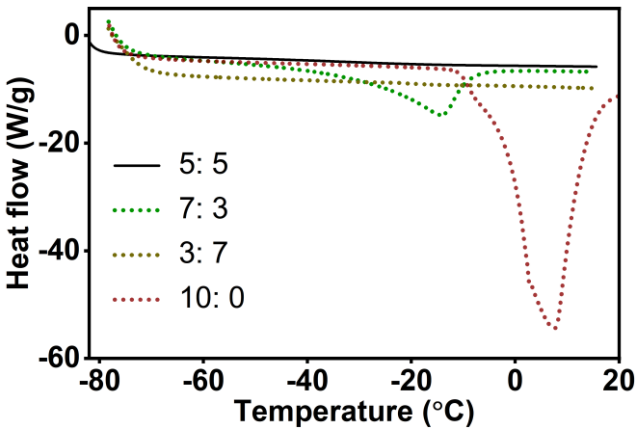

Fig. S21. DSC of H-MPA with different ratios of H_2O and DMSO.

Table S1. Comparison of the performances of the flexible H-MPA-based epidermal sensor with other reported conductive hydrogel-based sensors.

Materials	Human motion detection (-30 ℃)	Human motion detection (25 ℃)	Sensing range (-30 ℃)	GF (-30 ℃)	Sensing range (25 ℃)	GF (25 ℃)	Reference
H-MPA	Yes	Yes	250%	1.25	1000%	1.41	This work
PAA- ChCl-[EMIM]Cl	Yes	Yes	--	--	500%	0.17	[1]
PAA-rGO-Ga^{3+}	--	Yes	--	--	400%	1.77	[2]
PHEA-MXene-Ca^{2+}	--	Yes	--	--	400%	1.73	[3]
PHEA-agarose-[EMIM]Cl	--	Yes	--	--	700%	0.93	[4]
PAM-PVA-PVBIMBr	Yes	Yes	--	--	800%	1.22	[5]
PAM-SA-Ca^{2+}	--	Yes	--	--	1700%	0.081	[6]

PAM-CCS-Na^{+}	--	Yes	--	--	1100%	0.214	[7]
PAM-CNF-CS	--	Yes	--	--	200%	3.13	[8]
PAM-CCNF-PEDOT:PSS	--	Yes	--	--	837%	0.31	[9]
PANi/PVA/GA	--	Yes	--	--	100%	1.2	[10]
PVA-PAA-Fe^{3+}	--	Yes	--	--	1400%	0.12	[11]
PVA-CNF	Yes	Yes	--	--	660%	1.5	[12]
PVA-SNF-CN	--	Yes	--	--	585.8%	0.74	[13]
PVA-G-PDA-AgNPs	--	Yes	--	--	330%	0.724	[14]
Gelatin-Na_3Cit	--	Yes	--	--	525%	1.5	[15]

References

1. K. Xue, C. Shao, J. Yu, H. Zhang, B. Wang, W. Ren, Y. Cheng, Z. Jin, F. Zhang and Z. Wang, *Adv. Funct. Mater.*, 2023, **33**, 2305879.
2. Z. Zhang, L. Tang, C. Chen, H. Yu, H. Bai, L. Wang, M. Qin, Y. Feng and W. Feng, *J. Mater. Chem. A*, 2021, **9**, 875-883.
3. N. Li, X. Wang, Y. Liu, Y. Li, J. Li, Z. Qin and T. Jiao, *Chem. Eng. J.*, 2024, **483**, 149303.
4. J. Sun, G. Lu, J. Zhou, Y. Yuan, X. Zhu and J. Nie, *ACS Appl. Mater. Interfaces*, 2020, **12**, 14272-14279.
5. T. Lei, J. Pan, N. Wang, Z. Xia, Q. Zhang, J. Fan, L. Tao, W. Shou and Y. Gao, *Mater. Horiz.*, 2024, **11**, 1234-1250.
6. H. Sun, K. Zhou, Y. Yu, X. Yue, K. Dai, G. Zheng, C. Liu and C. Shen, *Macromol. Mater. Eng.*, 2019, **304**, 1900227.
7. H. Ding, X. Liang, Q. Wang, M. Wang, Z. Li and G. Sun, *Carbohydrate Polymers*, 2020, **248**, 116797.
8. J. Yu, Y. Feng, D. Sun, W. Ren, C. Shao and R. Sun, *ACS Appl. Mater. Interfaces*, 2022, **14**, 10886-10897.
9. Z. Bian, Y. Li, H. Sun, M. Shi, Y. Zheng, H. Liu, C. Liu and C. Shen, *Carbohydrate Polymers*, 2023, **301**, 120300.
10. Y. Zhao, B. Zhang, B. Yao, Y. Qiu, Z. Peng, Y. Zhang, Y. Alsaid, I. Frenkel, K. Youssef, Q. Pei and X. He, *Matter*, 2020, **3**, 1196-1210.
11. S.-H. Shin, W. Lee, S.-M. Kim, M. Lee, J. M. Koo, S. Y. Hwang, D. X. Oh and J. Park, *Chem. Eng. J.*, 2019, **371**, 452-460.
12. Y. Ye, Y. Zhang, Y. Chen, X. Han and F. Jiang, *Adv. Funct. Mater.*, 2020, **30**, 2003430.
13. S. Bao, J. Gao, T. Xu, N. Li, W. Chen and W. Lu, *Chem. Eng. J.*, 2021, **411**, 128470.
14. L. Fan, J. Xie, Y. Zheng, D. Wei, D. Yao, J. Zhang and T. Zhang, *ACS Appl. Mater. Interfaces*, 2020, **12**, 22225-22236.

15. Z. Qin, X. Sun, H. Zhang, Q. Yu, X. Wang, S. He, F. Yao and J. Li, *J. Mater. Chem. A*, 2020, **8**, 4447-4456.